Quantitative mRNA imaging throughout the entire *Drosophila* brain

Xi Long[1], Jennifer Colonell[2], Allan M Wong[3], Robert H Singer[1,4] & Timothée Lionnet[1,5]

We describe a fluorescence *in situ* hybridization method that permits detection of the localization and abundance of single mRNAs (smFISH) in cleared whole-mount adult *Drosophila* brains. The approach is rapid and multiplexable and does not require molecular amplification; it allows facile quantification of mRNA expression with subcellular resolution on a standard confocal microscope. We further demonstrate single-mRNA detection across the entire brain using a custom Bessel beam structured illumination microscope (BB-SIM).

Brain development and function require the expression of select genes at specific times in appropriate neurons. Because of the wealth of genetic tools available, *Drosophila* has emerged as an important model system for identifying the gene networks underlying neuron types and functions[1–3]. Existing approaches that quantify gene expression using sequencing methods mainly rely on isolated cell populations, in which neurons are extracted from their native context. RNA fluorescence *in situ* hybridization (FISH) is a powerful technique that allows measurement of mRNA levels with subcellular resolution within preserved tissue[4–6], but its application to adult *Drosophila* brains has proved difficult owing to limited probe penetration and sample autofluorescence. Here we develop a simplified, robust whole-mount RNA FISH method for adult *Drosophila* brains that connects gene expression with neuronal identity and functional anatomy. Whole-mount imaging is advantageous as compared to sectioning-based methods because it does not require extensive sample preparation (serial sectioning, labeling, mounting, imaging) or post-imaging analysis (stitching, registration). By optimizing processing and clearing, we demonstrate whole-brain multiplexed mRNA quantification using a standard confocal microscope. Upon imaging with a custom Bessel beam structured illumination microscope, individual mRNA molecules can be detected and counted throughout the entire cleared brain.

An overview of the method is shown in **Figure 1a**. To facilitate probe penetration, we treated the tissue with 5% acetic acid[7] and applied a high-temperature (50 °C) incubation to enhance diffusion, before lowering the temperature to 37 °C for efficient hybridization. To improve the signal–to-noise ratio, we quenched the autofluorescence using sodium borohydride and optically cleared the tissue with xylene. (**Supplementary Fig. 1**). The method did not require molecular amplification, could be performed in 2 d, and was compatible with immunostaining (**Supplementary Fig. 2**). A stepwise protocol and comparison with pre-existing approaches are described in the **Supplementary Protocol**, **Supplementary Note 1** and **Supplementary Figure 1**.

To validate the specificity of our approach, we compared wild-type with transgenic flies in which GFP was expressed in neurons expressing pigment-dispersing factor (PDF). PDF neurons are part of the circadian pacemaker network and consist of two groups, four large ventrolateral neurons (l-LNvs) and four small ventrolateral neurons (s-LNvs), in each hemisphere[8]. Brains labeled with FISH probes targeting GFP and PDF mRNAs with different dyes were imaged on a confocal microscope and revealed the characteristic two groups of l-LNvs and s-LNvs on each side of the brain. GFP-coding mRNA signal was not observed outside of the PDF neurons or in wild-type flies, confirming the specificity of the hybridization (**Fig. 1b**).

To determine whether we could resolve lower-abundance mRNAs, we probed *timeless* (*tim*) mRNA, which codes for a transcription factor that cycles daily[9] and regulates the circadian cycle. We acquired confocal images of wild-type files entrained at zeitgeber times (ZT) 2 and 14, and we observed a strong *tim* signal in PDF neurons at ZT14, whereas the intensity was much lower at ZT2, consistent with previous reports (**Fig. 1c**,**d** and **Supplementary Fig. 3**)[10,11].

Because of its multiplexing potential, the technique lends itself to multiple applications. FISH can be a powerful characterization and validation tool for the rapidly expanding collections of genetic lines used in neuroscience and optogenetics. Three split-Gal4 fly lines with expression in cell types (Mi1, Mi4, Mi9)[12] with known neurotransmitter expression (F.P. Davis, S.R. Eddy and G.L. Henry, personal communication) were crossed with the UAS-myr::HaloTag line to generate expression of a HaloTag reporter in the desired neurons[13]. The HaloTag protein was labeled with a fluorescent ligand (Online Methods), and FISH probes were simultaneously hybridized to mRNAs from genes involved in distinct neurotransmitter pathways (Gad1, vGlut and Chat, associated with GABAergic, glutamatergic and cholinergic transmission, respectively) labeled with three different dyes. The overlap between the neurons containing the HaloTag and those with the FISH signals confirmed the expected neurotransmitter signatures (**Supplementary Fig. 4**). We then interrogated the expression of the three genes associated with distinct neurotransmitter pathways.

[1]Transcription Imaging Consortium, Howard Hughes Medical Institute Janelia Research Campus, Ashburn, Virginia, USA. [2]Applied Physics and Instrumentation Group, Howard Hughes Medical Institute Janelia Research Campus, Ashburn, Virginia, USA. [3]Fly Functional Connectome, Howard Hughes Medical Institute Janelia Research Campus, Ashburn, Virginia, USA. [4]Department of Anatomy and Structural Biology, Dominick P. Purpura Department of Neuroscience, Gruss Lipper Biophotonics Center, Albert Einstein College of Medicine, Bronx, New York, USA. [5]Institute for Systems Genetics, Department of Cell Biology, New York University Langone Medical Center, New York, New York, USA. Correspondence should be addressed to T.L. (lionnett@janelia.hhmi.org) or X.L. (longx@janelia.hhmi.org).

RECEIVED 22 DECEMBER 2016; ACCEPTED 28 APRIL 2017; PUBLISHED ONLINE 5 JUNE 2017; DOI:10.1038/NMETH.4309

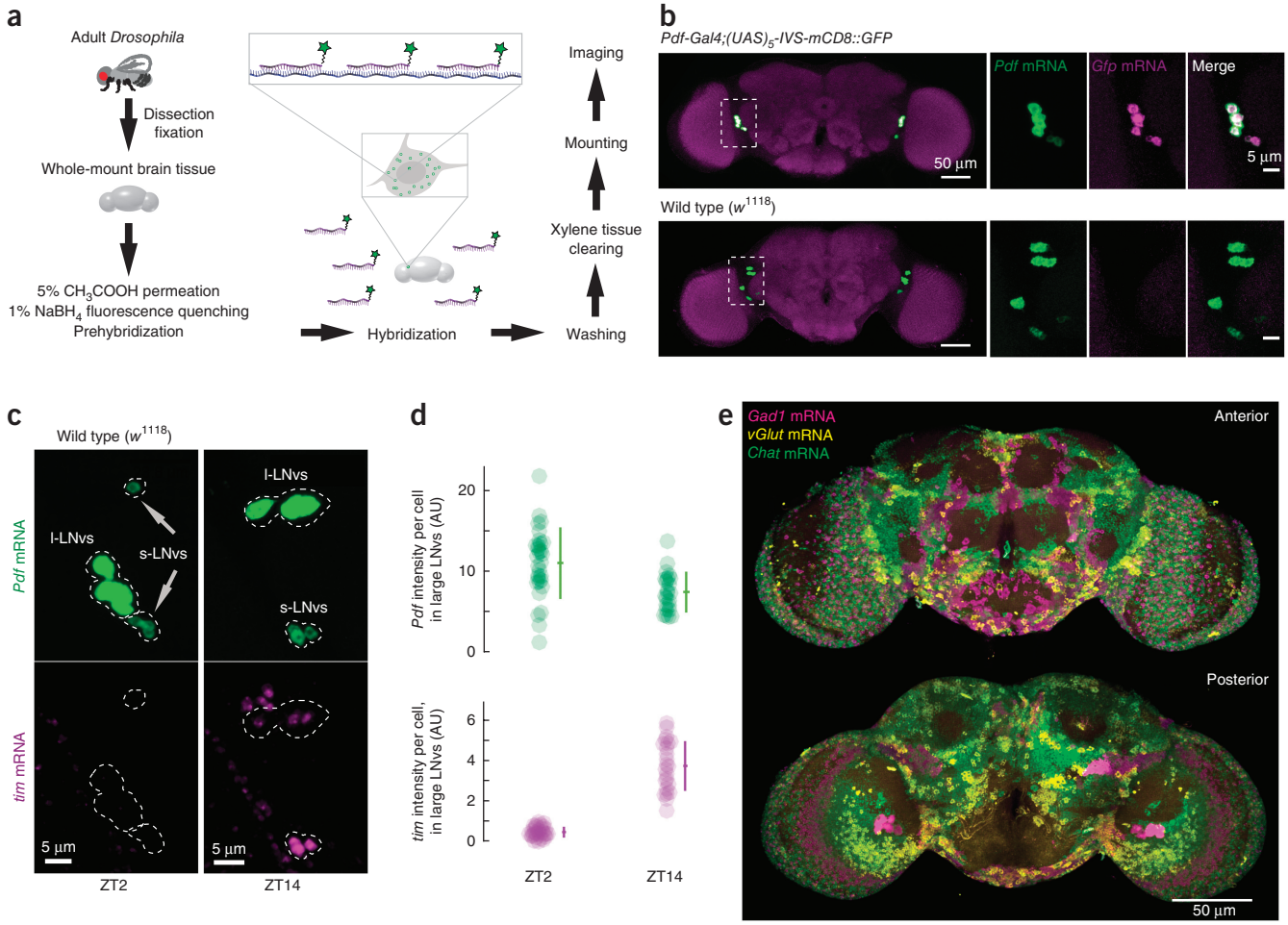

Figure 1 | mRNA quantification in whole-mount *Drosophila* brains using a confocal microscope. (**a**) Schematic illustration of the RNA FISH workflow. (**b**) Simultaneous detection of *Pdf* mRNA (green) and *Gfp* mRNA (magenta) using confocal microscopy. Images are maximum-intensity projections. Top, a *Pdf-Gal4;(UAS)$_5$-IVS-mCD8::GFP* fly brain; *Pdf* and *Gfp* mRNAs colocalize. Bottom, a wild-type fly brain. Only endogenous *Pdf* expression was detected; *Pdf* expression is lower in the s-LNvs (faint cells). (**c**) Comparison of *tim* (magenta) expression at ZT2 (left) and ZT14 (right) in wild-type PDF neurons (green). Images are maximum-intensity projections of confocal microscope stacks. Dashed lines indicate the outline of the PDF neuron cell bodies. (**d**) Quantification of *tim* expression in PDF l-LNvs neurons at ZT14 and ZT2. *tim* expression is reduced at ZT2, while *Pdf* expression shows little change over the daily cycle (N = 3 brains for ZT2, 4 for ZT14; mean ± s.d. shown for each condition). AU, arbitrary units. (**e**) Simultaneous detection of *Gad1* (magenta), *vGlut* (yellow) and *Chat* (green) mRNAs in a whole-mount *Drosophila* adult brain. Top, anterior, and bottom, posterior views of a confocal stack (see **Supplementary Video 1** for 3D rendition and **Supplementary Fig. 5** for a close-up).

Resulting confocal stacks (**Fig. 1e**, **Supplementary Video 1**) display non-overlapping spatial patterns of expression, suggesting minimal coexpression of these neurotransmitters (**Supplementary Fig. 5**). Such multiplexing experiments provide a rapid, powerful tool to link gene expression patterns to brain-wide architecture, function and connectomics.

mRNA localization has been proposed to regulate local translation, particularly in neurons[14]. However, this remains mostly untested in animals because single-mRNA imaging in the large volumes relevant to tracing neuronal connections *in vivo* is challenging. Hence, we sought to detect the location of single molecules in whole-mount tissue. We built a custom Bessel beam selective plane illumination microscope, engineered to image in medium matched to the measured refractive index (RI) of xylene-cleared *Drosophila* tissue, to avoid aberration and scattering. The thin light sheet provides axial resolution of 0.3 µm, ~3× better than that of confocal microscopy. Excitation through two orthogonally mounted objectives allows structured illumination (SIM) resolution enhancement for lateral resolution of 0.2 µm. (**Fig. 2a**, **Supplementary Fig. 6**, Online Methods, **Supplementary Note 2**)[15].

The multiple nascent pre-mRNAs at the locus of a transcribing gene typically generate a bright nuclear focus when imaged with FISH[4]. We imaged various fly lines differing in the location or number of genomic insertions of a GFP reporter gene (all under the control of a *Pdf* driver). Lines harboring the reporter gene in a single insertion site (attP2 or attP18) displayed zero or one bright focus in each of the PDF neurons, but never two foci per nucleus (**Fig. 2b**). In contrast, flies with the reporter gene in two insertion sites (attP18; attP2) frequently displayed two foci per nucleus. Only transcriptionally active alleles should give rise to visible nuclear foci by FISH. Indeed, the probability of observing *tim* nuclear foci in s-LNvs increased fivefold between ZT2 and ZT14, whereas the probability of observing *Pdf* foci displayed little variation (**Supplementary Fig. 7**). These results agree with findings that *tim* transcription is reduced at ZT2, while *Pdf* transcription does not substantially change over the daily cycle[11].

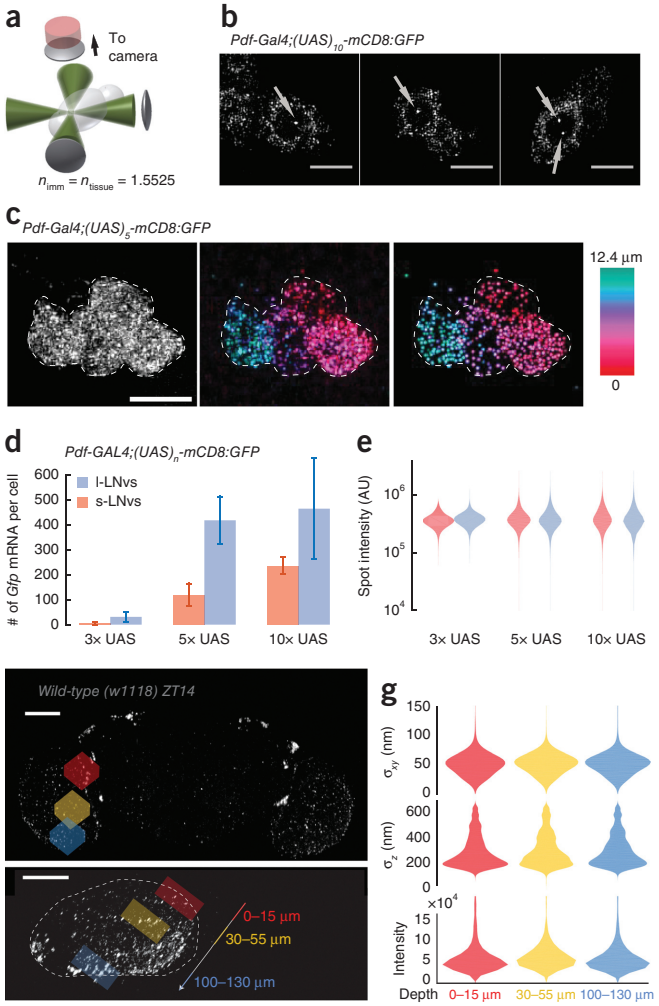

Figure 2 | Single-mRNA detection in whole-mount *Drosophila* brains. (**a**) Schematic of Bessel beam structured illumination (BB-SIM) microscope. A thin, patterned light sheet (green) may be formed in the sample using either of two excitation objectives. The excitation objectives, sample, and detection objective are all immersed in imaging medium whose refractive index (*n*) is matched to that of the xylene-cleared tissue. (**b**) PDF neurons in fly lines with different genomic insertions of a GFP reporter gene. Left and center, single genomic insertion, one nuclear focus; right, double genomic insertion, two nuclear foci. Images are maximum-intensity projections of confocal stacks; arrows mark transcription sites. (**c**) Single *Gfp* mRNAs appear as diffraction-limited spots in PDF neurons within whole-mount *Drosophila* adult brain. Left, *Pdf* mRNA signal used as a marker for the cell bodies; center, *Gfp* mRNA signal color-coded for depth; right, reconstructed image obtained using a spot counting algorithm, color-coded for depth (key at right). (**d**) *Gfp* mRNAs per cell in fly lines in which the GFP reporter is driven by 3, 5, or 10 UAS repeats ($N = 3, 4, 4$ brains, respectively; mean ± s.d.). Large and small PDF neurons (l-LNvs and s-LNvs) are color-coded blue and red, respectively. (**e**) Intensities of *Gfp* mRNA spots in 3× UAS, 5× UAS and 10× UAS lines. (**f**) Representation of the three optic lobe regions used to compare the detection performance. Images are maximum-intensity projects of transcription site containing slices from BB-SIM stacks; arrows mark transcription sites. Top, anterior view; bottom, sagittal view. (**g**) Spot intensity and size as a function of depth in high-resolution scans of the three regions of the optic lobe labeled in **f** using probes against the *tim* mRNA.

In order to detect single molecules, flies with the *Pdf-Gal4* reporter expressing GFP in PDF neurons were hybridized with probes targeting the *Pdf* and the *Gfp* transcripts in separate colors, and high-resolution BB-SIM volumes containing the PDF neurons were acquired (**Fig. 2c**), revealing diffraction-limited foci of the GFP-encoding mRNAs in the PDF neuron cell bodies. Individual endogenous *Pdf* mRNAs within the cell bodies were too dense to be resolved as individual molecules (left panel in **Fig. 2c**). Using an algorithm to characterize the individual spots[16], the brightness of the mRNAs typically appeared as a unimodal intensity distribution above the fluorescent background (**Supplementary Fig. 8**), consistent with individual mRNAs. A characteristic of single-mRNA detection is that the intensity of detected mRNAs remains constant regardless of the expression level. To demonstrate this, we used a set of reporter lines with increasing number of upstream activating sequence (UAS) elements upstream of the GFP reporter, generating increasing levels of GFP expression in the PDF neurons[17] (**Supplementary Fig. 9**). When imaging those brains at high resolution (**Fig. 2d**), lines with increasing number of UAS elements displayed an increased number of spots per cell; importantly, the brightness of individual spots did not vary, confirming detection of individual molecules (**Fig. 2e**).

Tissue thickness can decrease detection efficiency because of aberrations and scattering. To assess the impact of tissue depth on detection performance, we imaged the distribution of fluorescence intensities and spot sizes of *tim* mRNAs in different brain regions. Spot intensities and sizes were constant through the entire brain sample, suggesting that depth had a minimal impact on detection quality (**Fig. 2f**,**g**, **Supplementary Fig. 8g**).

We demonstrated the potential of the technique by quantifying the absolute expression of *tim* in PDF neurons at ZT2 and ZT14 (**Fig. 3a**,**b**). These results are in agreement with confocal measurements of total intensity (**Fig. 1d** and **Supplementary Fig. 3**) and previous findings[11]. They provide the basis for absolute gene expression studies at the scale of the entire brain.

While most PDF mRNAs localized to neuronal cell bodies, some molecules were visible in processes (**Fig. 3c**–**f**). PDF mRNA levels decreased with increasing distance from cell bodies, which is similar to what is observed in mammalian neurons in culture[14]. Interestingly, the distribution of PDF mRNAs along processes differed between s-LNvs and l-LNvs. However, this difference was not observed for mRNAs of a control transgene, suggesting cell-type-specific regulation of localization (**Fig. 3f** and **Supplementary Fig. 10**).

Whole-mount mRNA FISH enables the interrogation of gene expression levels at the single-cell level using a standard confocal microscope. Because of its simplicity and versatility (it is multiplexable and compatible with HaloTag labeling and immunofluorescence), we expect this to constitute an important tool for addressing the cellular and molecular basis of brain function. When combined with high-resolution microscopy, whole-mount mRNA FISH can detect and count individual molecules within an intact entire brain. This permits visualizing neuronal architecture and connections simultaneously with the levels and localization of mRNA expression. Whole-mount smFISH could be extended through spectral or sequential barcoding in order to multiplex large numbers of mRNA species in each sample[6,18,19]. Combined with the powerful genetic tools inherent to *Drosophila*, this technique is a unique tool to address questions such as the role of mRNA localization in memory formation.

METHODS

Methods, including statements of data availability and any associated accession codes and references, are available in the online version of the paper.

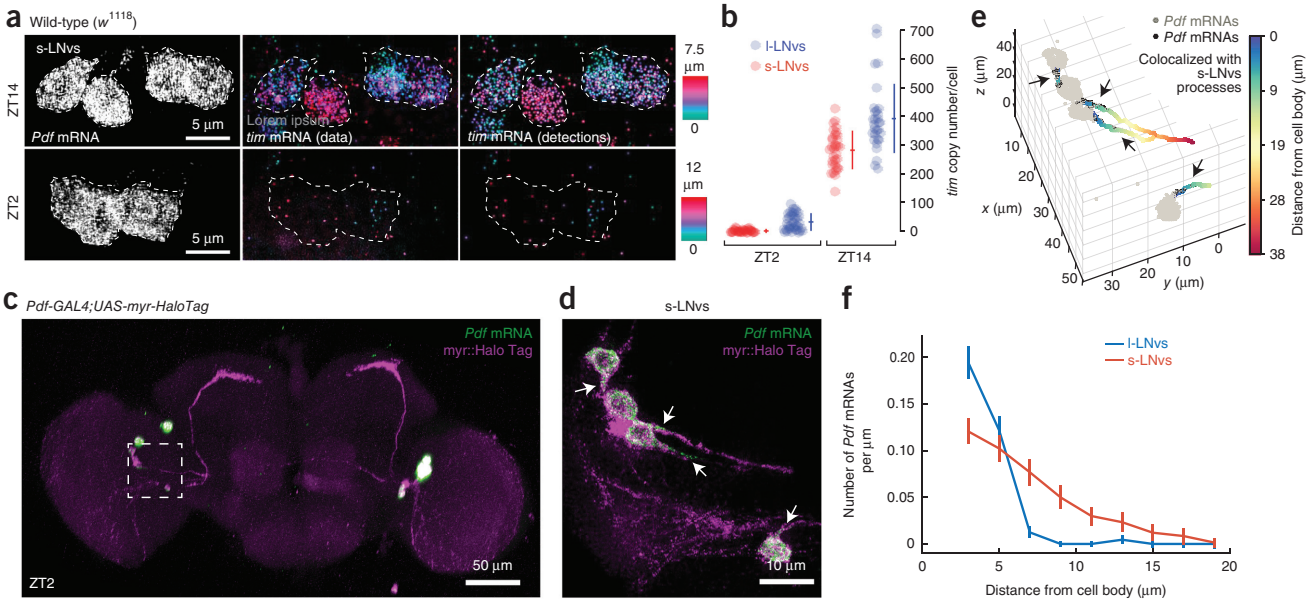

Figure 3 | Spatiotemporal regulation of mRNA expression in whole-mount *Drosophila* brains. (**a**) PDF neurons display numerous single *tim* mRNAs at zeitgeber time (ZT) 14 (top) while *tim* expression is reduced at ZT2 (bottom) in PDF s-LNvs neurons. Left, maximum-intensity projections of BB-SIM stacks of the *Pdf* mRNA FISH channel are used to mark the cell bodies; center, color-coded projections of the *tim* mRNA FISH channel BB-SIM stacks; right, color-coded projection of the *tim* mRNA image reconstruction obtained using spot-counting algorithm. (**b**) Quantification of the number of *tim* mRNAs in PDF neurons at ZT14 and ZT2. Large and small PDF neurons (l-LNvs and s-LNvs) are color-coded blue and red, respectively. $N = 5$ brains for ZT2, 4 brains for ZT14; mean ± s.d. shown for each condition. (**c**) Correlation of neuronal architecture with gene expression localization. Maximum-intensity projection of the BB-SIM stack of a brain in which the PDF neurons are filled with a fluorescent HaloTag ligand (myr::HaloTag, purple) and the *Pdf* mRNA is imaged by FISH (green). (**d**) High-resolution scan of the boxed region in **c** displaying four s-LNvs. *Pdf* mRNAs (green) accumulate within the cell bodies and in the proximal region of the processes (arrows). (**e**) Localization analysis of the data shown in **d**: *Pdf* mRNAs detected are represented by light gray spots; *Pdf* mRNAs that localize with processes are indicated by black spots and their prominent locations highlighted with arrows. Processes emanating from the s-LNVs are color-coded for distance from the cell body. (**f**) Quantification of the density of *Pdf* mRNA molecules at ZT 2 in PDF neuron processes as a function of distance from the cell body, showing a PDF cell-type-specific localization profile (5 brains totaling 35 l-LNvs, 36 s-LNvs with, respectively, 23 and 37 traced processes; mean ± s.e.m. assuming Poisson counting error).

Note: Any Supplementary Information and Source Data files are available in the online version of the paper

Note added in proof: While this paper was in review, a complementary technique appeared in a preprint by Yang et al.[20].

ACKNOWLEDGMENTS

We thank members of the former Transcription Imaging Consortium, M. Rosbash, M. Diaz, K. Abruzzi, L. Lavis, T. Brown, U. Heberlein, T. Harris and Y. Wu, for valuable suggestions. We are grateful to A. Nern for providing the Mi4, Mi1 and Mi9 transgenic flies and to G. Henry and F. Davis for providing transcriptome profiling information. We thank K. Close for assistance with *Drosophila* dissections and A. Lemire, L. Wang, R. Ray, K. Aswath and X. Zhang for assistance with molecular biology and characterizing transgenic flies. We also thank E. Betzig J. Jordan, and D. Milkie for consultation on the design of the BB-SIM microscope and the control software for the system; L. Shao for structured illumination analysis code; and A. Taylor for assistance with confocal imaging. Funding for this work was provided by the Howard Hughes Medical Institute.

AUTHOR CONTRIBUTIONS

X.L. and T.L. designed the experiments and wrote the manuscript. X.L. performed the experiments and did confocal measurements. J.C. designed and built the Bessel beam SPIM with SIM microscope and performed measurements using it. X.L., J.C. and T.L. analyzed the data. A.M.W. created the transgenic flies for detecting two GFP transcription sites and contributed to the neurotransmitter experiments. R.H.S. consulted on the research and helped to write the manuscript. All authors edited the manuscript.

COMPETING FINANCIAL INTERESTS

The authors declare competing financial interests: details accompany the online version of the paper.

1. Henry, G.L., Davis, F.P., Picard, S. & Eddy, S.R. *Nucleic Acids Res.* **40**, 9691–9704 (2012).
2. Jenett, A. *et al. Cell Rep.* **2**, 991–1001 (2012).
3. Knowles-Barley, S., Longair, M. & Armstrong, J.D. *Database (Oxford)* **2010**, baq005 (2010).
4. Femino, A.M., Fay, F.S., Fogarty, K. & Singer, R.H. *Science* **280**, 585–590 (1998).
5. Raj, A., van den Bogaard, P., Rifkin, S.A., van Oudenaarden, A. & Tyagi, S. *Nat. Methods* **5**, 877–879 (2008).
6. Shah, S., Lubeck, E., Zhou, W. & Cai, L. *Neuron* **92**, 342–357 (2016).
7. Fernández, J. & Fuentes, R. *Dev. Dyn.* **242**, 503–517 (2013).
8. Helfrich-Förster, C. & Homberg, U. *J. Comp. Neurol.* **337**, 177–190 (1993).
9. Hughes, M.E., Grant, G.R., Paquin, C., Qian, J. & Nitabach, M.N. *Genome Res.* **22**, 1266–1281 (2012).
10. Zhao, J. *et al. Cell* **113**, 755–766 (2003).
11. Abruzzi, K.C. *et al. PLoS Genet.* **13**, e1006613 (2017).
12. Strother, J.A. *et al. Neuron* **94**, 168–182.e10 (2017).
13. Kohl, J. *et al. Proc. Natl. Acad. Sci. USA* **111**, E3805–E3814 (2014).
14. Buxbaum, A.R., Wu, B. & Singer, R.H. *Science* **343**, 419–422 (2014).
15. Planchon, T.A. *et al. Nat. Methods* **8**, 417–423 (2011).
16. Lionnet, T. *et al. Nat. Methods* **8**, 165–170 (2011).
17. Pfeiffer, B.D. *et al. Genetics* **186**, 735–755 (2010).
18. Chen, K.H., Boettiger, A.N., Moffitt, J.R., Wang, S. & Zhuang, X. *Science* **348**, aaa6090 (2015).
19. Levsky, J.M., Shenoy, S.M., Pezo, R.C. & Singer, R.H. *Science* **297**, 836–840 (2002).
20. Yang, L. *et al.* Preprint at https://doi.org/10.1101/128785 (2017).

ONLINE METHODS

Protocol availability. A detailed step-by-step instruction is provided as a **Supplementary Protocol** and is also accessible from *Protocol Exchange*[21].

***Drosophila* brain tissue and preparation.** The Pdf-GAL4 fly line was from Renn *et al.*[22]; pJFRC4-3XUAS-IVS-mCD8::GFP, pJFRC5-5XUAS-IVS-mCD8::GFP and pJFRC2-10XUAS-IVS-mCD8::GFP were from Pfeiffer *et al.*[17]. Mi1 (*55C05-p65ADZp(attP40);71D01-ZpGdbd(attP2))*, Mi4 (*48A07-p65ADZp(attP40);79H02-ZpGdbd(attP2))* and Mi9 (*48A07-p65ADZp(attP40);VT046779-ZpGdbd(attP2))* split-GAL4 driver lines are described in Strother *et al.*[12]. UAS-myr::HaloTag was from Kohl *et al.*[13]. We used w^{1118} flies that were otherwise wild type or *timeless* experiments. To generate the PDF-GFP titration flies, we crossed Pdf-GAL4 to stocks that contained 3×, 5×, or 10× UAS-IVS-mCD8::GFP. For the double GFP insertion line, we made a stock of pJFRC2-10XUAS-IVS-mCD8::GFP(attp18)::pJFRC2-10XUAS-IVS-mCD8::GFP(attp2). The stock was then crossed to Pdf-Gal4. To generate selective expression of a HaloTag reporter in specific neurons of the optic lobe, we crossed Mi1, Mi4, Mi9 to UAS-myr::HaloTag. Flies were reared on standard cornmeal/agar media supplemented with yeast under 12 h light/12 h dark cycles at 25 °C. Male flies were used in circadian experiments, female flies otherwise (see **Supplementary Table 1**). 3-to-5-day-old adult flies were collected, then dissected in phosphate-buffered saline (PBS) and fixed in 2% paraformaldehyde for 55 min at 25 °C under normal lighting. For ZT14 samples, brain tissues were dissected under red LED lighting. The brain tissues underwent dehydration before they were stored in 100% EtOH overnight. When comparing conditions, sample sizes were chosen to be at least 3 brains per condition. Quantitative data analysis was performed without blinding or randomization.

FISH. Amino-labeled oligonucleotide probes[5] (Biosearch Technologies) were labeled to NHS-ester fluorophores according to manufacturer's guidelines. To perform FISH, rehydrated *Drosophila* brain tissues were exposed to 5% acetic acid at 4 °C for 5 min. After being fixed in 2% paraformaldehyde for 55 min at 25 °C, the tissues were incubated in 1× PBS with 1% of $NaBH_4$ at 4 °C for 30 min and then in pre-hybridization buffer (15% formamide, 2× SSC, 0.1% Triton X-100) for 2 h at 50 °C. The brain tissues were transferred to 50 µL of hybridization buffer (10% formamide, 2× SSC, 5× Denhardt's solution, 1 mg/ml yeast tRNA, 100 µg/ml, salmon sperm DNA, 0.1% SDS) with FISH probes (50–100 ng/µL per reaction, containing probe sets against one or multiple genes) and incubated at 50 °C for 10 h and then at 37 °C for an additional 10 h. After a series of wash steps, the brain tissues were dehydrated and introduced to xylene for tissue clearing. A detailed description of the FISH procedures is provided as a **Supplementary Protocol**.

HaloTag staining and IHC. The brains of flies expressing the HaloTag reporter were stained with HaloTag-JF646 during fixation. After dissection, brain tissues were transferred to 2% paraformaldehyde containing 2 µM of HaloTag-JF646 (ref. 23). They were then incubated with agitation for 55 min at 25 °C, followed by a series of 1× PBS washes. Antibody staining was performed after the FISH labeling. After a series of wash steps, the brain tissues were blocked with 10% normal goat serum (NGS) in 1× PBS with 0.5% Triton X-100 (0.5% PBT) at room temperature for 2 h, followed by overnight primary antibody staining at 4 °C. The primary and secondary antibody solutions contained 5% NGS in 0.5% PBT. For GFP primary antibody staining, the tissues were exposed to 1:1000 rabbit polyclonal anti-GFP Fraction (Life Technologies A11122); for PDF primary antibody staining, the tissues were exposed to 1:1000 mouse anti-PDF (Developmental Studies Hybridoma Bank, PDF C7); for nc82 primary staining, the tissues were exposed to 1:30 mouse anti-bruchpilot (Developmental Studies Hybridoma Bank, nc82). After washing the primary antibody, brain tissues were incubated in secondary antibody overnight at 4 °C. For GFP secondary antibody staining, the tissues were exposed to 1:1000 AF488 goat anti-rabbit (Invitrogen A11034). For PDF and nc82 secondary antibody staining, the tissues were exposed to 1:1000 Cy3 AffiniPure Goat anti-mouse (Jackson ImmunoResearch 115-165-166). Brain tissues were then fixed in 2% paraformaldehyde for 55 min at 25 °C before dehydration and xylene clearing.

Confocal imaging. For confocal imaging, all brain tissues were attached to poly-L-lysine coated cover glass and mounted in DPX (Janelia Adult *Drosophila* CNS DPX mounting protocol). We used a Zeiss LSM 880 confocal microscope (561 nm and 633 nm laser lines) imaged through a 25× DIC NA 0.8 oil objective to detect GFP transcripts in Pdf-Gal4;JFRC5 constructs and wild-type flies (**Fig. 1**). Images were acquired with sequential excitation as stacks with 1.5 µm *z*-spacing. Detector gain and laser power were kept constant for all samples. To detect *Gfp* transcripts in the UAS titration experiments, we used a Zeiss LSM 800 confocal microscope (561 nm and 633 nm laser lines) imaged through a 63× DIC NA 1.4 oil objective. Images were acquired with sequential excitation as stacks with 1.0-µm *z*-spacing. Detector gain and laser power were kept constant for all samples. To detect the overlapping neurotransmitter expression in Gal4 lines, we used a Zeiss LSM 880 confocal microscope (488 nm, 561 nm and 633 nm laser lines) imaged through a 63× DIC NA 1.4 oil objective with hyperspectral lambda detection scan with 1.00 µm *z*-spacing. The multiplex neurotransmitter images were acquired on a Zeiss LSM 880 confocal microscope (488 nm, 561nm and 633 nm laser lines) imaged through a 25× DIC NA 0.8 oil objective. Images were acquired with hyperspectral lambda detection scan as stacks with 0.50 µm *z*-spacing. Summary of imaging parameters are in **Supplementary Table 1**.

BB-SIM imaging. The BB-SIM images were acquired on a custom-built microscope, which is further described in **Supplementary Note 1**. Two orthogonally mounted excitation objectives are used to form Bessel beams, which are stepped to create an illumination sheet periodically striped along *x* or *y*, while a third objective (optical axis along the *z* direction) detects fluorescence (**Fig. 2a**). The objectives and sample are immersed in imaging media (90% 1,2-dichlorobenzene, 10% 1,2,4-trichlorobenzene) with refractive index = 1.5525, matched to the cleared tissue. To employ structured illumination analysis, we collect multiple images with the illumination stripe pattern shifted to tile the plane in *x*, and repeat the process orthogonally to tile the plane in *y*. The sample is then

moved in *z*, and the imaging repeated, and so on to image the 3D volume. In this work, we collected 11 images (phases) in *x* and *y*, setting the annulus aperture to achieve a FWHM of the beam intensity profile of 350 nm at the waist. The resolution after SIM analysis, measured on fluorescent beads with 560 nm excitation, is 200 × 200 × 290 nm (FWHM). Sample treatment is identical to that for confocal samples through the clearing step. After clearing, the samples are mounted on 1.5 × 3 mm polylysine-coated coverslips, and held in xylene until imaging.

Image analysis. Image analysis details are discussed in **Supplementary Note 3**.

Code availability. Image analysis code will be made available on github: https://github.com/timotheelionnet/Long_Drosophila_mRNA_Analysis.

Data availability. Probe sequences are listed in **Supplementary Table 2**. All other data are available from the authors on reasonable request.

21. Long, X., Coloness, J., Wong, A.M., Singer, R.S. & Lionnet, T. *Protocol Exchange* http://dx.doi.org/10.1038/protex.2017.051 (2017).
22. Renn, S.C.P., Park, J.H., Rosbash, M., Hall, J.C. & Taghert, P.H. *Cell* **7**, 791–802 (1999).
23. Grimm, J.B. *et al. Nat. Methods* **12**, 244–250 (2015).

doi:10.1038/nmeth.4309